Journal of Alloys and Compounds, 184 (1992) 1–9
JALCOM 164

Synthesis, characterization and hydrogenation behaviour of Mg–$x$wt.%FeTi(Mn) and La_2Mg_{17}–$x$wt.%$LaNi_5$ – new hydrogen storage composite alloys

P. Mandal, K. Dutta and K. Ramakrishna
Department of Physics, Banaras Hindu University, Varanasi 221 005 (India)

K. Sapru
Technology Innovation Products, Troy, MI 48098 (USA)

O. N. Srivastava
Department of Physics, Banaras Hindu University, Varanasi 221 005 (India)

(Received August 7, 1991)

Abstract

New hydrogen storage materials with higher capacity and better suited for applications have been successfully synthesized. The hydriding behaviour of the new composite materials, Mg–$x$wt.%FeTi(Mn) and La_2Mg_{17}–$x$wt.%$LaNi_5$, were studied for various values of x ($x = 10$, 20, 30, 40 and 50). The Mg–x%FeTi(Mn) materials were activated under a hydrogen atmosphere (about 33 kgf cm^{-2}) and an optimum storage capacity of about 3.5 wt.% corresponding to room temperature hydrogenation was established for $x = 40$. This high storage capacity – almost double the storage capacity of the well-known FeTi(Mn) – has been observed under ambient conditions. The La_2Mg_{17}–x%$LaNi_5$ materials were activated at higher temperatures (about 360 °C) in a hydrogen atmosphere. An optimum storage capacity of 4 wt.% in terms of pressure and composition was observed for La_2Mg_{17}–20%$LaNi_5$ at 350 °C. In comparison with the native ingredient La_2Mg_{17}, much faster (nearly three times) kinetics were found. In order to understand the hydrogenation behaviour and the high storage capacity, structural–microstructural and chemical analyses of these composite materials were carried out. From the structural investigations it has been found that all the synthesized materials are multiphase. The composite material Mg–FeTi(Mn) was found to contain $FeTi_{1-x}$, magnesium, titanium and Ti–Mg phases. The higher storage capacity (about 3.5 wt.%) in the case of Mg–40%FeTi(Mn) is probably due to FeTi–Mg complexes. The hydrogen molecule is split at the FeTi surface and diffuses into the magnesium matrix via FeTi. In the case of La_2Mg_{17}–x%$LaNi_5$, the composite material consists of La_2Mg_{17}, $MgNi_2$, nickel and $LaNi_3$ phases. Because of the presence of nickel and nickel-containing phases (*e.g.* Mg–Ni), it is assumed that the dissociation of hydrogen is easier and hence the system La_2Mg_{17}–x%$LaNi_5$ has better kinetics than its counterpart La_2Mg_{17} alone.

1. Introduction

Recent events highlighting the vulnerability and unstable price of the premier fossil fuel (oil) have once again brought into focus the need for an appropriate substitute. Hydrogen is known to be a potential non-polluting

0925-8388/92/$5.00

renewable substitute and reversible hydrogen storage materials—the hydrides—are important ingredients in realizing this substitution. The promise possessed in regard to hydrogen storage behaviour by some intermetallics capable of providing hydrogen–hydride fuel have prompted explorations of several reversible hydrogen storage intermetallics such as FeTi, $LaNi_5$, $MmNi_5$ and Mg_2Ni [1–5]. However, there is an ongoing search for reversible hydrides with higher hydrogen storage capacity so as to obtain an appropriate weight–energy ratio. So far, investigations of hydrogen storage materials have centred on individual intermetallics capable of reversible hydrogenation behaviour. Recently, however, there have been some investigations which suggest that mixed-type composite materials may possess better hydriding characteristics [6, 7]. Such studies are rather sparse and, in order to test the viability of composite materials for hydrogen storage, further investigations are required. Magnesium has the highest storage capacity (about 7 wt.%) but is not a practical material since it does not form reversible hydrides [8, 9]. However, intermetallics such as Mg_2Ni and La_2Mg_{17} possess the potential for high storage capacity [10, 11]. Studies of composite materials involving magnesium or magnesium-bearing intermetallics may lead to new hydrogen storage materials with better hydriding characteristics.

In the present investigation we have undertaken studies on such composite hydrogen storage materials. Earlier we studied the hydrogen storage systems FeTi(Mn) [12] and La_2Mg_{17} [13] and, keeping in view the foregoing characteristics, we have now investigated Mg–$x$wt.%FeTi(Mn) and La_2Mg_{17}–$x$wt.%$LaNi_5$. Both these systems possess characteristics which are superior to the individual storage systems alone. For Mg–x%FeTi(Mn) it has been found that for $x = 40$ the storage capacity corresponds to 3.5 wt.%, which is almost double the storage capacity of about 1.9% for FeTi(Mn). After two cycles of initial activation at 400 ± 10 °C, the composite alloy Mg–x%FeTi(Mn) undergoes hydrogenation under ambient conditions. For the La_2Mg_{17}–20wt.%$LaNi_5$ system, in contrast to La_2Mg_{17}, a storage capacity of about 4 wt.% is reproducibly obtainable. In addition to this, La_2Mg_{17}–20%$LaNi_5$ shows kinetics (desorption rate) about three times faster than the corresponding rate for La_2Mg_{17}.

2. Experimental details

The native ingredients (FeTi–Mn, La_2Mg_{17}) were first prepared by melting a stoichiometric mixture of the individual elements. High purity iron (99.9%), titanium and manganese (99.99%) were mixed in the correct proportions, pressed into pellet form (1 cm × 2 cm) to get an alloy with the stoichiometry $Fe_{46}Ti_{50}Mn_4$ and melted in an r.f. induction furnace under an argon atmosphere in a previously outgassed graphite crucible. The initially prepared ingot was melted repeatedly to achieve homogeneity. La_2Mg_{17} was synthesized by a somewhat new synthesis route involving encapsulation of the subliming component magnesium. Pellets were prepared in such a way that the magnesium

was surrounded by lanthanum powder on all sides. The pellets were melted in a silica tube under an argon atmosphere. During the melting process water was circulated around the silica tube to avoid contamination of the silica by the alloy constituents, particularly magnesium and iron. This encapsulation method appears to be superior in the sense that when the pellets are melted, there is practically no magnesium loss [13]. In the next synthesis step the composite alloys Mg–$x$wt.%FeTi(Mn) were prepared by the encapsulation method. The composite material thus prepared was melted two or three times to obtain better homogeneity. The composite materials La_2Mg_{17}–$x$wt.%$LaNi_5$ were prepared by r.f. melting of a homogeneous mixture of La_2Mg_{17} and $LaNi_5$ in the correct stoichiometric ratios.

3. Results and discussion

3.1. Mg–xwt.%FeTi(Mn)

The hydrogenation behaviour of Mg–$x$wt.%FeTi(Mn) has been studied by monitoring pressure–composition isotherms. For all the composite alloys, desorption isotherms have been measured by the displacement method (volumetric) [14] in order to find the weight percentage of hydrogen in these materials. Since the as-synthesized Mg–x%FeTi(Mn) sintered alloys do not absorb hydrogen at room temperature, they were first activated by heating the material to about 400 °C in a hydrogen atmosphere. Heating was continued for 3–4 h under a hydrogen pressure of about 30 atm. For the second and subsequent cycles no activation through heat treatment was required for absorption–desorption. To find the optimum hydrogen storage capacity of these materials, several hydrogenation (absorption and desorption) runs have been performed at room temperature on activated samples. From the pressure–composition isotherms of Mg–x%FeTi(Mn) for several values of x ($x = 10$, 20, 30, 40 and 50) it has been found that Mg–40wt.%FeTi(Mn) has the maximum storage capacity. Figure 1 shows a representative desorption isotherm of Mg–40%FeTi(Mn) measured at room temperature. The maximum hydrogen storage capacity obtained in the present investigation has been found to correspond to about 3.6 wt.%. For other compositions, as the magnesium content of the system increases, the storage capacity and the rate of desorption have been found to decrease.

It may be pointed out that as the FeTi(Mn) content increases, the composite material becomes very brittle and after hydrogenation it breaks into homogenized powder consisting of fine particles of different phases. From the hydrogenation studies it appears that the presence of FeTi, $FeTi_2$ and magnesium-related phases plays a crucial role in acceleration of the hydriding characteristics. The composite material corresponding to Mg–40%FeTi(Mn) undergoes hydrogenation–dehydrogenation under ambient conditions and gives rise to a highest hydrogen storage capacity of about 3.5 wt.% for this system.

In order to understand the high storage capacity of Mg–x%FeTi(Mn), we explored the structural and microstructural characteristics of the composite

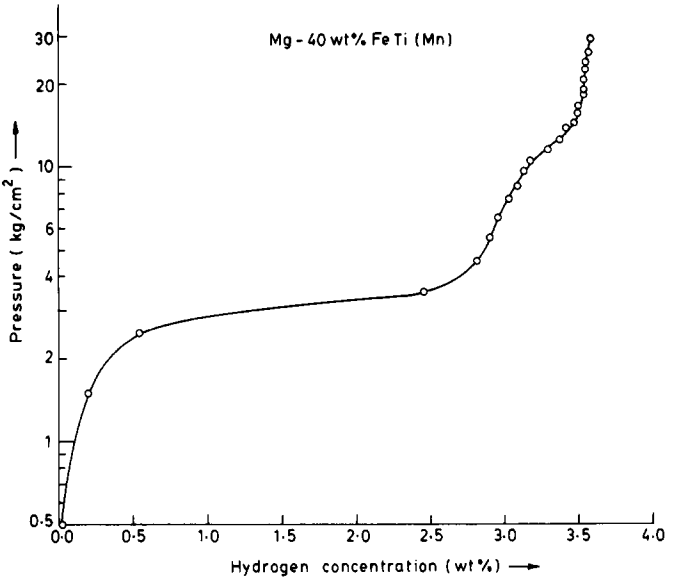

Fig. 1. Pressure–composition isotherm of Mg–40wt.%FeTi(Mn) composite alloy at room temperature.

material. X-ray diffraction (XRD) analysis was carried out using a Philips PW-1710 diffractometer. The XRD results for Mg–$x$wt.%FeTi(Mn) with $x = 10$, 20, 30, 40 and 50 revealed that the as-synthesized material is a multiphase one exhibiting FeTi(Mn), magnesium, titanium and Ti–Mg. (From here on we shall omit (Mn); when we write FeTi, the presence of small quantities of manganese is implicit.) The synthesis process presumably leads to some loss of titanium, resulting in the formation of $FeTi_{1-x}$, titanium and Ti–Mg. Figures 2(a) and 2(b) exhibit representative XRD patterns of the as-synthesized material. $FeTi_{1-x}$ (approximately FeTi) and magnesium are found to be the majority phases, titanium and Ti–Mg [15] the minority phases. In the initial stages of hydrogenation the XRD pattern did not undergo any discernible change. It can thus be assumed that in the early stages of activation of the material the dominant hydrogenation and storage capacity arises from the hydrogenation of FeTi and possibly magnesium in the presence of FeTi, titanium and Ti–Mg. In order to gain further insight into the structural–microstructural characteristics, we carried out scanning electron microscopy (SEM) investigations coupled with energy-dispersive analysis by X-rays (EDAX). Figure 3 is a representative SEM picture (secondary electron image) of as-synthesized Mg–x%FeTi(Mn). This micrograph corresponds to $x \approx 40$, the composition which exhibited the highest hydrogen storage capacity of 3.6 wt.%. SEM coupled with EDAX showed that the dominant microstructural feature corresponded to Mg–x%FeTi where magnesium particles are surrounded by FeTi matrix or FeTi is situated on top of magnesium clusters, *i.e.* the configuration corresponds to FeTi–Mg. From the observed results

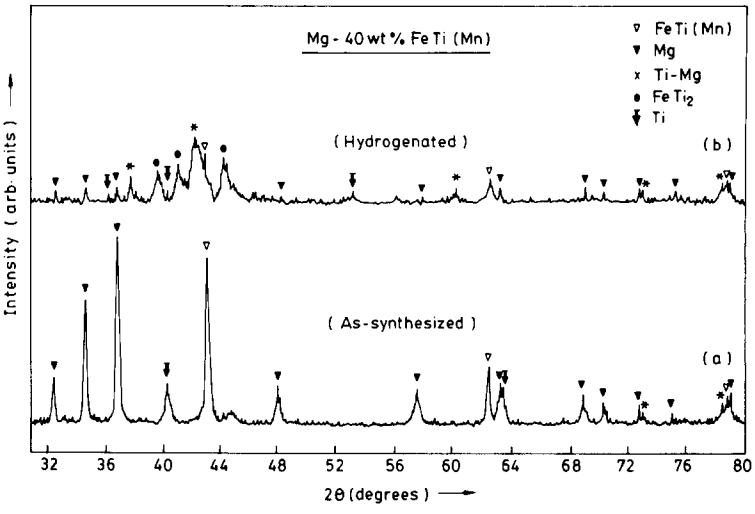

Fig. 2. Representative X-ray powder diffraction pattern of (a) as-synthesized and (b) hydrogenated (after several hydrogen absorption–desorption cycles) Mg–$x$wt.%FeTi(Mn) composite material. Formation of a mixture of different phases is indicated.

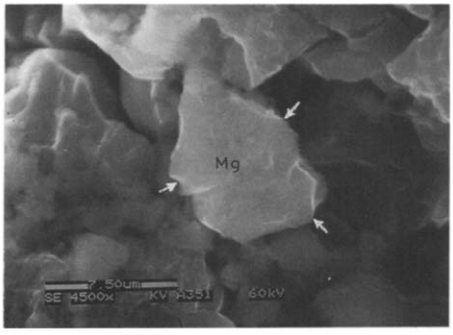

Fig. 3. Representative scanning electron micrograph of cross-section of as-synthesized Mg–$x$wt.%FeTi(Mn) alloys showing magnesium matrix surrounded by FeTi grains.

on enhanced hydrogen capacity coupled with the observed microstructural features, it seems evident that in the presence of FeTi the hydrogenation may commence with FeTi but it embodies magnesium as well, whose hydrogenation temperature is lowered in the presence of FeTi. On the basis of the observed structural and microstructural characteristics, it appears that the hydrogenation characteristics of the FeTi–Mg complex may start with the splitting of H_2 into H atoms on the FeTi surface. The H atoms may then diffuse into magnesium via FeTi, leading eventually to saturation of the FeTi–Mg complex. Since, in addition to FeTi, magnesium is also involved, the storage capacity is expected to be higher. Thus the observed optimum storage capacity of about 3.6 wt.% for Mg–40wt.%FeTi as against about 1.9 wt.% for FeTi alone appears explicable. As regards the optimum capacity

at about 40 wt.% FeTi, it appears that for $x > 40$ the hydrogenation behaviour and capacity will be dominated by FeTi and for $x < 40$ the hydrogenation of magnesium present in the Mg–x%FeTi may not be optimum.

3.2. La_2Mg_{17}–$x$wt.%$LaNi_5$

The hydriding behaviour of La_2Mg_{17}–$x$wt.%$LaNi_5$ ($x = 10$, 20, 30, 40 and 50) was studied using a volumetric method similar to that followed for Mg–FeTi. The as-synthesized samples were activated by applying a hydrogen pressure of 33 kg cm^{-2} and heating to 360 ± 10 °C for about 6 h. Since desorption in this case, unlike Mg–FeTi, was negligible at room temperature, the desorption for La_2Mg_{17}–20wt.%$LaNi_5$ was carried out at higher temperatures. Figure 4 shows a representative desorption isotherm of La_2Mg_{17}–20%$LaNi_5$ measured at 350 ± 10 °C. This temperature was found to be optimum with regard to the capacity and plateau pressure of La_2Mg_{17}–20%$LaNi_5$. From the pressure–composition (P–C) isotherm it is clear that the maximum weight percentage of hydrogen desorbed from this material is about 4.03%. From this figure it may be noted that the P–C isotherm of the La_2Mg_{17}–20%$LaNi_5$ composite material consists of two plateaux. This suggests that the as-synthesized composite alloy comprises two kinds of reversible hydrogen storage phases. Further, it has been found that addition of 20% $LaNi_5$ to La_2Mg_{17} accelerates the hydriding rate by about three times in comparison with La_2Mg_{17} alone.

In order to understand the role of $LaNi_5$ addition, which significantly accelerated the hydrogen desorption rate of La_2Mg_{17}, analysis of the phases in the La_2Mg_{17}–20%$LaNi_5$ composite material and microstructural observations of the alloys were undertaken. These studies confirm that the hydriding rate

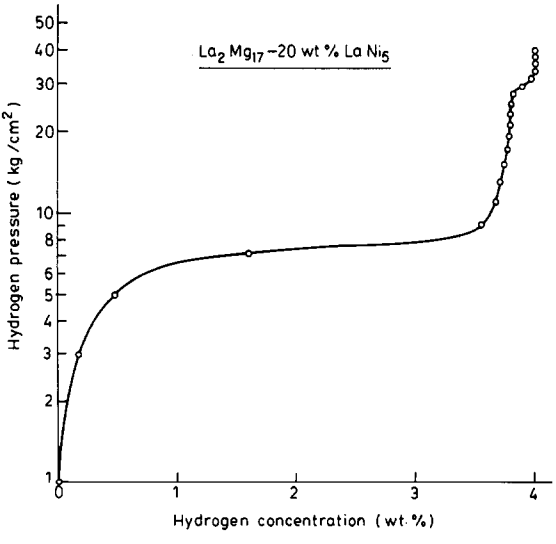

Fig. 4. Pressure–composition isotherm of La_2Mg_{17}–20wt.%$LaNi_5$ composite material at 350 °C.

and hydrogen storage capacity are closely related to the microstructure and the types of phases present in the alloy. Figure 5 shows a representative XRD pattern of as-synthesized La_2Mg_{17}–20wt.%$LaNi_5$. Analysis of the XRD pattern revealed that the dominant phase present in the composite alloy was La_2Mg_{17}. However, a few diffraction peaks representative of $LaNi_3$, $MgNi_2$ and nickel phases also appeared. As is known, the presence of nickel on the surface decreases the activation energy of dissociation of H_2 molecules and hence leads to faster kinetics. The rapidity with which the present composite alloy absorbs hydrogen seems to suggest that besides nickel, the additional phases, particularly those embodying nickel, may also affect the kinetics (absorption–desorption). Thus the free nickel and nickel-containing phases are expected to play a crucial role in the acceleration of the hydriding rate of the composite alloy. Figure 6 is a representative SEM image of the as-synthesized composite material La_2Mg_{17}–20wt.%$LaNi_5$. This micrograph shows the multiphase nature of the material, thus confirming the XRD results already described. Presumably the larger crystallites represent the main

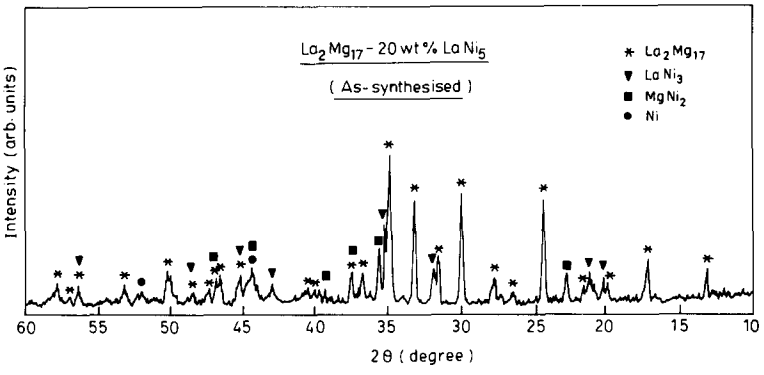

Fig. 5. X-ray diffraction pattern of as-synthesized La_2Mg_{17}–20wt.%$LaNi_5$ composite alloy representing a multiphase material. Different phases are outlined.

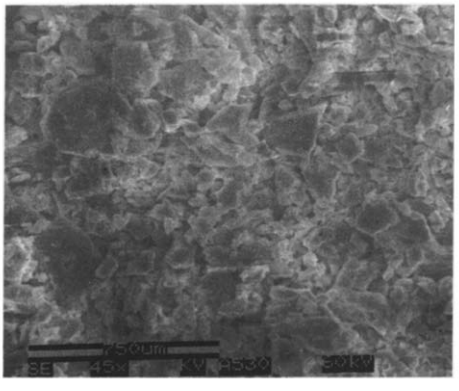

Fig. 6. Representative scanning electron micrograph of as-synthesized La_2Mg_{17}–20wt.%$LaNi_5$ showing the presence of a mixture of different phases.

La_2Mg_{17} matrix while the smaller precipitate-like particles correspond to the minority phases such as $MgNi_2$, $LaNi_3$ and free nickel. Explorations in various regions of the specimen through EDAX revealed that, in addition to La_2Mg_{17}, nickel either embodied in $MgNi_2$ or in the free form appears to be invariably present. This would imply that compared to La_2Mg_{17} alone the multiphase composite material formed through melting of La_2Mg_{17}–20wt.%$LaNi_5$ would have a better dissociation of H_2 molecules and hence faster kinetics. Thus the observed faster kinetics seem to be explicable.

4. Conclusions

The hydrogenation behaviour of the new composite materials Mg–$x$wt.%FeTi(Mn) and La_2Mg_{17}–$x$wt.%$LaNi_5$ ($x = 10$, 20, 30, 40 and 50) was studied. The optimum hydrogen storage capacity in relation to its reversible characteristic has been found to be about 3.5 wt.% under ambient conditions for Mg–40%FeTi(Mn), which is double the storage capacity of the intermetallic FeTi(Mn) alone (about 1.9 wt.%). A storage capacity of 4 wt.% is reproducibly obtained for La_2Mg_{17}–20%$LaNi_5$ and much faster hydrogen absorption–desorption rates are found than for La_2Mg_{17}. The structural–microstructural characteristics of these new storage materials were examined by X-ray diffraction, electron microscopy and chemical analysis. In the case of Mg–40%FeTi(Mn), $FeTi_{1-x}$ and magnesium were found to be majority phases and titanium and Ti–Mg minority phases. The higher storage capacity obtained in this case may be due to the absorption of hydrogen by FeTi–Mg complexes. Dissociation of H_2 is expected to take place at the FeTi surface and then diffusion takes place into the magnesium matrix via FeTi. For La_2Mg_{17}–20%$LaNi_5$, La_2Mg_{17} and $MgNi_2$ were found to be the majority phases and nickel and nickel-containing alloys the minority ones. The presence of free nickel and nickel-containing materials presumably accelerates the hydrogen absorption–desorption, leading to the better kinetics observed for La_2Mg_{17}–x%$LaNi_5$.

Acknowledgments

We are grateful to Dr. K. V. C. Rao for several illuminating discussions. The present work was financially supported by the Department of Non-conventional Energy Sources, Government of India, New Delhi.

References

1 J. J. Reilly and R. H. Wiswall Jr., *Inorg. Chem.*, *7* (1968) 2254.
2 H. Nagai, H. Kitagaki and K. Shoji, *Trans. Jpn. Inst. Met.*, *29* (1988) 494.
3 J. H. N. Van Vucht, F. A. Kuijpers and H. C. A. M. Bruning, *Philips Res. Rep.*, *25* (1970) 133.

4 E. L. Huston and G. D. Sandrock, *J. Less-Common Met.*, *74* (1980) 435.
5 P. Shen, Y. Zhang, S. Chen and J. Zhou, *Chem. J. Chinese Univ.*, *6*(3) (1985) 197.
6 B. Tanguy, J. L. Soubeyroux, M. Pezat, J. Portier and P. Hagenmuller, *Mater. Res. Bull.*, *11* (1976) 14441.
7 H. Nagai, H. Tomizawa, T. Ogarawara and K. Shoji, *J. Less-Common Met.*, *157* (1990) 15.
8 F. H. Ellinger, C. H. Holly Jr., B. B. McInteer, D. Pavone, R. M. Potter, E. Staritzy and W. H. Zacharlasen, *J. Am. Chem. Soc.*, *77* (1955) 2647.
9 J. J. Reilly and R. H. Wiswall Jr., *Inorg. Chem.*, *7* (1968) 2254.
10 Z. Yunshi, J. Jianhua, Y. Huatang, Chen Shengchang, W. Da and Z. Taoshi, *J. Mater. Res.*, *5* (1990) 1431.
11 M. Khrussanova, M. Pezat, B. Darriet and P. Hagenmuller, *J. Less-Common Met.*, *86* (1982) 153.
12 P. Mandal, K. Ramakrishna and O. N. Srivastava, *Int. J. Hydrogen Energy*, in preparation.
13 K. Dutta and O. N. Srivastava, *Int. J. Hydrogen Energy*, *15* (1990) 341.
14 K. Ramakrishna, S. K. Singh, A. K. Singh and O. N. Srivastava, in R. P. Dahiya (ed.), *Progress in Hydrogen Energy*, Vol. 7, Riedel, Boston, MA, 1987, p. 81.
15 C. Suryanarayana and F. H. Froes, *J. Mater. Res.*, *5* (1990) 1880.